Aalborg Universitet

AALBORG UNIVERSITY
DENMARK

Evaluation of the battery degradation factors for nano-satellites at LEO

Knap, Vaclav; Kjelgaard Vestergaard, Lars; Gismero, Alejandro; Stroe, Daniel-Ioan

Published in:
Proceedings of the 71st International Astronautical Congress

Publication date:
2020

Document Version
Version created as part of publication process; publisher's layout; not normally made publicly available

IAC-20-C3,3,6,x56704

Evaluation of the battery degradation factors for nano-satellites at LEO

Vaclav Knap[a,b,c,*], Lars Vestergaard[a], Alejandro Gismero[c] and Daniel-Ioan Stroe[c]

[a] *GomSpace A/S, 9220 Aalborg East, Denmark,* vakn@gomspace.com
[b] *Faculty of Electrical Engineering, Czech Technical University in Prague, 166 27 Prague, Czech Republic*
[c] *Department of Energy Technology, Aalborg University, 9220 Aalborg East, Denmark*
* Corresponding Author

Abstract

Mission design and spacecraft design are challenging activities, which have to be carefully conducted in order to achieve a successful mission for a nano-satellite. In NewSpace, especially in the area of nano-satellites, there is a strong drive towards agile and quickly market deployed products. Typically, commercial-off-the-shelf (COTS) batteries are used and their manufacturers rarely provides specifically needed information about them. Thus, it is necessary for the nano-satellite developer to assess the battery performance and lifetime, on their own, in order to support an accurate mission/spacecraft design. In the proposed approach, the possible degradation factors and their feasible ranges were firstly considered, in order to limit the test requirements, and the selected degradation tests were performed. The scope of battery performance indicators analysis was limited to battery capacity and resistance. Their change and sensitivity were evaluated in relation to calendar aging, considering temperature and state-of-charge factors, and to cycling aging, considering temperature and cycle depth factors, and to radiation aging. Afterwards, the identified degradation rates were used for lifetime modelling. The resulting lifetime model had 0.69% and 0.81% root-mean-square-error, compared to the experiment, for the prediction of capacity and resistance, respectively.
Keywords: battery; cubesat; degradation; lifetime; model; nano-satellite

1. Introduction

Lithium-ion (Li-ion) batteries currently represent the energy storage technology of choice for small satellite solutions [1]. Their task is to provide power to satellite load without interruption in moments when power generation from solar panels is not sufficient. Since satellites at low Earth orbit (LEO) revolve typically around Earth 11-16 times per day, they pass through eclipse periods, when they are obscured from Sun. In these cases, the power generation from solar panels is practically zero, and all the consumption has to be supplied from batteries. Consequently, batteries are required to provide sufficient amount of power and energy throughout the entire mission. However, due to degradation, battery capability to store energy and to provide power decays. Therefore, an appropriate design of the spacecraft, mission and battery solution is needed.

Li-ion battery degradation is a non-linear phenomenon, depending on various factors [2]. Thus, the degradation factors and their significance have to be identified. It is a common practise to perform lifetime tests related to a specific application (e.g. mobile phones [3], electric vehicles [4], stationary grid energy storage [5]). General requirements for batteries in LEO satellites were summarized by Borthomieu [6] to be 2-15 years life duration; 5500 charge/discharge cycles per year; one cycle lasts 90 minutes, typically 60 minutes charging and 30 minutes discharging; the cycle depth is between 10-40% state-of-charge (SOC) depending on the mission duration; charging rates around 0.3 C-rate and discharging rates around 0.5-0.7 C-rate. For nano-satellites, respective CubeSats, the character of orbits remains the same. However, some conceptual expectations are different. The development cycle of nano-satellites shall be shorter, cheaper and more flexible. The used batteries are primarily space qualified commercial off-the-shelf (COTS) products, originally intended for terrestrial applications, and not space grade batteries. The mission duration is expected to be shorter. Moreover, there are some technical implications of smaller spacecrafts (e.g. small thermal mass) [1]. A general guideline for battery life testing can be found in an ESA handbook [7]. There are proposed calendar and cycling tests, where cycling tests can be performed in a normal or an accelerated manner. In terms of space grade batteries, one can find manufacturers (e.g. Saft) that performs lifetime tests and provide those data for various conditions [8], [9]. However, for common COTS battery cells, only datasheets with basic lifetime information are available and the specific lifetime testing is left on a battery pack produced or a spacecraft developer. Tests conducted for various anonymized COTS cells for diverse conditions were presented by ABSL as a battery pack manufacturer [10], [11], [12], showing that the sensitivity on various degradation factors (e.g. cycle depth, charging cut-off voltage and temperature) varies from cell type to cell type. Thus, they need to be always performed for a specific technology.

In this work, one specific type of COTS Li-ion battery cell is used for degradation tests, considering calendar, cycling, and radiation aging. The capacity and resistance are the performance indicators, which are selected for analyses of the battery cell degradation. Their degradation rates are evaluated under exposure to various factors (i.e. temperature, SOC, cycle depth, etc.). Subsequently, the degradation results are used to parametrize a lifetime model that can predict the battery lifetime within the performed tests conditions.

2. Experiment

Battery testers Digatron 600, MACCOR Series 4000 and Neware 4000 were used for testing cylindrical 18650 cells (3000 mAh NanoPower Battery from GomSpace). The charging voltage cut-off limit is 4.2 V, the discharging voltage cut-off limit is selected to be 2.95 V, which corresponds to the base capacity of 2.75 Ah.

The testing procedure consisted of a reference performance test (RPT) and a degradation test, as illustrated in Fig. 1. The role of the RPT is to measure the actual performance indicators of the cells, such as capacity, resistance, and power capability. The complete RPT is depicted in Fig. 2, where the cell is firstly charged by constant current – constant voltage (CC-CV) by 1.5 A, to 4.0 V and 0.05 A, and then discharged by 1.5 A to 2.95 V to obtain the partial capacity. Secondly, the cell is charged by CC-CV, but this time to 4.2 V to obtain the full capacity from the consequent discharge. This is followed by charging the cell to 4.0 V, where a synthetic mission profile (SMP) [13] is performed, and afterwards the cell is fully charged. The pulse train procedure is then performed for 100, 80, 60, 40, 20 and 0% SOC and it consists of a set of charging and discharging pulses, each 20 second long, followed by 5 minutes relaxation for currents of 3, 1.5, 0.6 and 0.18 A. The RPT is performed always at the beginning-of-life (BOL) and then periodically thereafter during the degradation test. The degradation tests were performed to age the cells under specific conditions. Three types of degradations modes were considered: calendar, cycling, and radiation.

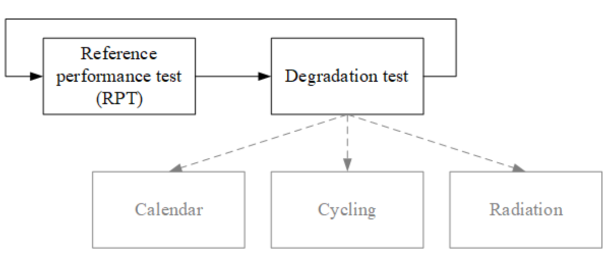

Fig. 1. Degradation test procedure

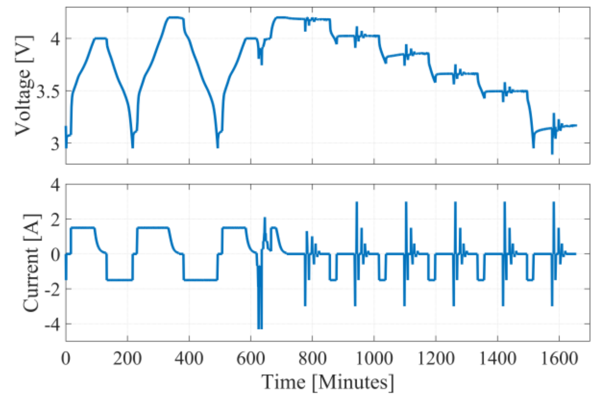

Fig. 2. Reference performance test (RPT)

2.1 Calendar degradation tests

The cells were stored at open-circuit conditions and once at two months an RPT is performed. Temperature and SOC dependencies were investigated. For investigating the effect of the temperature, the cells were always charged to 4.0 V (~75% SOC) and stored at 45, 25, 7.5, and -15°C. For investigating the the effect of the SOC, the cells were stored at 45°C and 100, 89, 75, 62% SOC, which corresponds to the charging voltage cut-off limits of 4.2, 4.1, 4.0 and 3.9 V, respectively.

2.2 Cycling degradation tests

The selected cycling tests conditions covered the dependencies of temperature and cycle depth. For the temperature influence study, the cells were cycled at 5, 25, and 45°C. The cycling profile was selected to be a SMP with an accelerating factor of two, in detail described in [13]. The cycle depth was 0.3 Ah and the cells were charged to 4.0 V.

The influence of cycle depth was studied by cycling the cells by 0.1, 0.2 and 0.4 Ah per cycle, which corresponds approximately to a SOC change of about 4, 7 and 15%, respectively. The cells were cycled at room temperature. The charging voltage limit was 4.0 V. The cycling current was selected in an acceleration manner to be 3 A for constant current discharge and 3A/0.2A for constant current – constant voltage charging.

2.3 Radiation degradation tests

The battery cells are expected to experience around 20 kRad total ionizing dose (TID) during their missions at LEO [1]. In order to investigate the influence of such TID amount on battery performance a group of cells were exposed to radiation and a control group was left at room temperature for the same amount of time between RPTs.

3. Lifetime analysis and modelling

Two battery cell performance indicators were selected for degradation analysis and lifetime modelling. The first is the total discharging capacity obtained during the RPT after charging the cell fully to 4.2 V and discharging by 0.5 C to 2.95 V. The second performance indicator is the resistance obtained after one second pulse of 3 A discharging current applied at 60% SOC. The capacity and resistance are normalized with respect of their initial values.

The calendar aging happens over time and the main occurring degradation process is the growth of a solid electrolyte interphase (SEI) layer for Li-ion batteries with a carbon-based anode. Cycling aging introduces additional processes to calendar aging, that are the results of ongoing (de-)intercalation mechanism, such as volume changing, SEI cracking, etc. Since the calendar degradation is present, while the cells are cycled, a calendar capacity loss/resistance growth model is used to extract the pure cycling contribution [14].

3.1.1 Calendar degradation modelling

Based on the literature [14] and experimental results, the calendar models are proposed as:

$$C_{cal} = n - \alpha_{cap} \cdot \sqrt{t} \quad (1)$$

$$R_{cal} = n + \alpha_{res} \cdot t^{0.75} \quad (2)$$

where C_{cal}/R_{cal} stands for calendar capacity/resistance and t is time in days. The fitting variable n is the initial normalized value of the quantity. It is expected to be equal to one, but it is allowed to be freely fitted in order to compensate for possible data discrepancy, $\alpha_{cap}/\alpha_{res}$ is capacity/resistance degradation rate for calendar aging.

3.1.2 Cycling degradation modelling

The cycling degradation expressions were established in a similar way as for the calendar degradation.

$$C_{cyc} = n - \beta_{cap} \cdot \sqrt{Q} \quad (3)$$

$$R_{cyc} = n + \beta_{res} \cdot Q \quad (4)$$

Where C_{cyc}/R_{cyc} stands for cycling capacity/resistance and Q is charging throughput expressed in Ah. β_{cap}/β_{res} is capacity/resistance degradation rate for cycling aging.

3.1.3 Composed degradation model

The capacity and resistance degradation from calendar and cycling aging is considered to be additive in this study, according to [14]. Thus, the formulation takes form:

$$C = 1 - \alpha_{cap} \cdot \sqrt{t} - \beta_{cap} \cdot \sqrt{Q} \quad (5)$$

$$R = 1 + \alpha_{res} \cdot t^{0.75} + \beta_{res} \cdot Q \quad (6)$$

4. Results

In this section, the experimental test results are summarized and analyzed, including evaluation of the degradation rates and the lifetime model.

4.1 Calendar aging

4.1.1 State-of-charge dependence

At high temperature (i.e. 45°C), the capacity fade seems to be not sensitive to the SOC level, as shown in Fig. 3(a), as the degradation rates are quite similar. It was expected that the highest degradation would be obtained at 100% SOC [15]; however, this is not the case from these tests, as the cells stored at 75% SOC exhibit the highest degradation rate.

On the other hand, there is a clear dependence of the resistance increase on the storage temperature as illustrated in Fig 3(b). The most demanding conditions are the high temperature (45°C) and the high SOC (100%).

The results demonstrate clearly that the degradation trajectory of the capacity fade and the resistance increase is independent. That has a further negative implication for any state-of-health estimation methods based on a fixed relation between the resistance and the capacity [16].

4.1.2 Temperature dependence

In the case of cells stored at 75% SOC and at various levels of temperature, there has been observed an exponential dependence of the capacity fade and the resistance increase on temperature, as shown in Fig. 4, which is in an agreement with Arrhenius' law.

The identified degradation rates and the interpolated surface used for the degradation model are summarized and shown in Fig. 5.

4.2 Cycling aging

In order to obtain the pure theoretical cycling contribution to degradation, the calendar lifetime model was used to subtract the calendar degradation contribution from the measured data obtained from cycling degradation tests.

4.2.1 Temperature dependence

Cycling the battery cells with the SMP with a low cycle depth of 0.3 Ah does not seem to cause any significant degradation, when performed at 5 and 25°C, as shown in Fig. 6. Only the elevated temperature 45°C, caused over 3% of capacity fade after 2000 Ah charging throughput, compared to the values below 0.5%, observed at the lower temperature cases. Regarding the resistance, such cycling at the lower temperature levels have not contributed to the increase, or more contrary it might have a slightly beneficial effect compared to just idling the cells. The cycling at 45°C clearly contributed to the resistance growth.

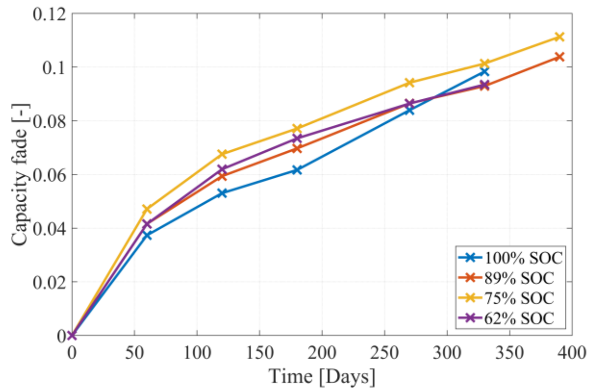

(a)

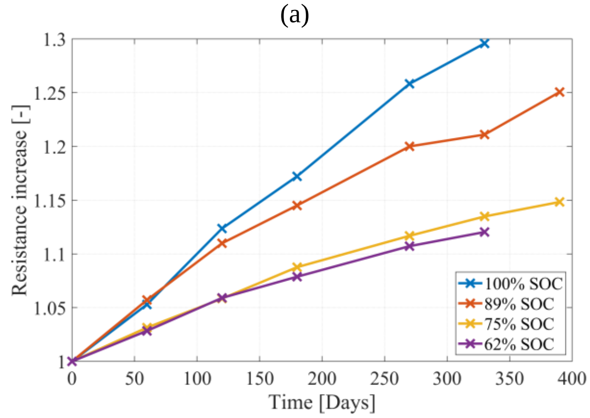

(b)

Fig. 3. Degradation results for calendar aging at 45°C and various SOC levels in terms of (a) capacity fade, and (b) resistance increase.

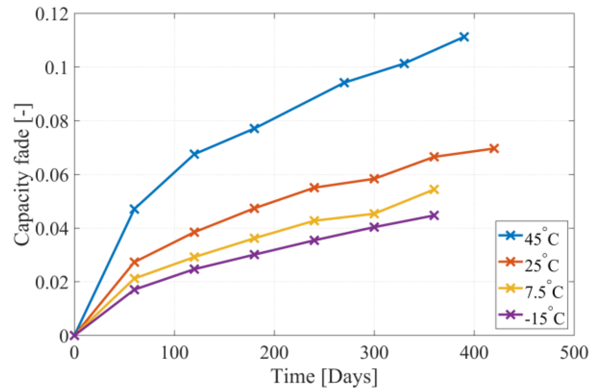

(a)

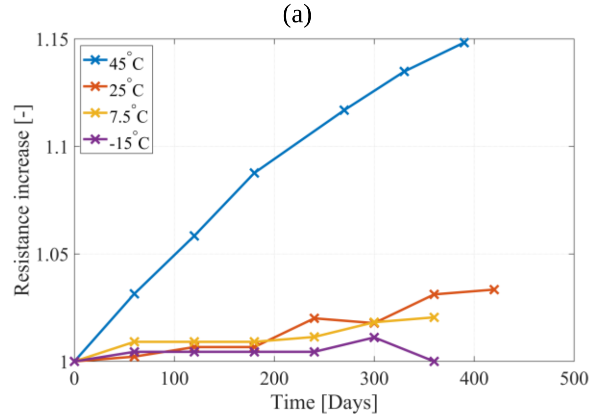

(b)

Fig. 4. Degradation results for calendar aging at 75% SOC and various temperature levels in terms of (a) capacity fade, and (b) resistance increase.

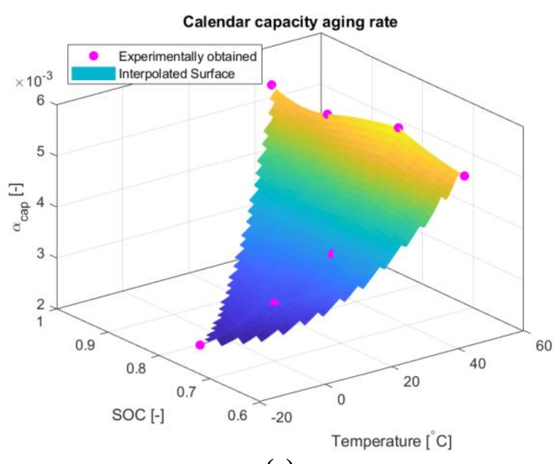

(a)

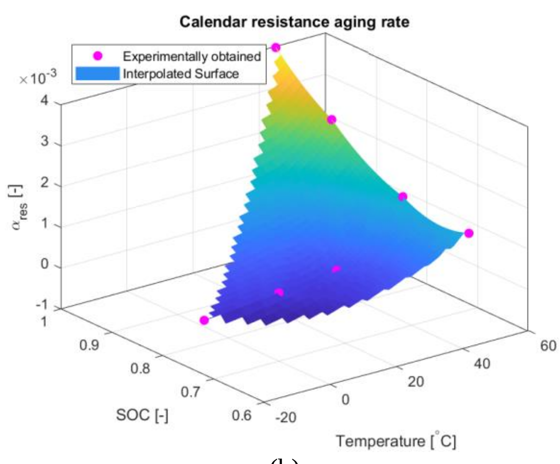

(b)

Fig. 5. Degradation (a) capacity and (b) resistance rate for calendar aging in relation to SOC and temperature.

4.2.2 Cycle depth dependence

The results, illustrated in Fig. 7, suggest that the capacity fade and resistance increase are only lightly dependent on shallow cycles with depths between 0.1 and 0.4 Ah. Furthermore, the capacity fade does not exhibit a monotonous dependence on the cycle depth. That can have a root in the cell behavior related to the sensitivity on SOC, as shown in Fig. 3(a), and in relation to cycling to a possibly an additional degradation factor of average cycle SOC.

The measured resistance increase presented a scattered behavior and no clear trend was observed. Thus, the contribution of low cycle depth cycling can be considered insignificant, similarly to the SMP cycling case at 25°C, discussed in Section 4.2.1.

The obtained cycling degradation rates are shown in Fig. 8. Temperature was identified as the aging factor that has the strongest impact on the cycling degradation of the studied Li-ion battery cells. Moreover, it can be observed from Fig. 8(a), that the degradation rate of SMP cycling is lower than the constant current cycling with 3 A charging and discharging current. The used SMP had the average amplitude discharging current of 1.2 A, and the average charging current amplitude was 0.6 A. Thus, it can be considered that the current amplitude has also a mild influence on the degradation rate. It causes either directly a higher stress, or it rises a cell's temperature, which then causes the additional degradation.

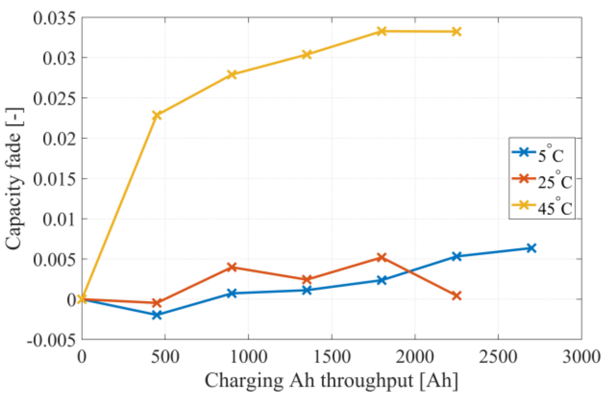

(a)

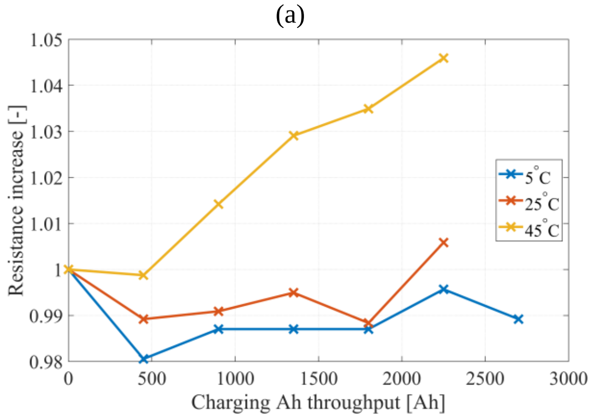

(b)

Fig. 6. Degradation results of (a) capacity fade, and (b) resistance increase for cycling aging dependent on temperature. The cells were cycled by the SMP with the cycle depth of 0.3 Ah.

4.3 Radiation aging

The influence of 20 kRad TID was investigated in this case. The results are shown in Fig. 9. All the cells had the identical capacity change after the test procedure. There is a minimal difference in the resistance change that could be caused by cell-to-cell variations, or a difference in a storage temperature (cells stored in the laboratory vs. cells being transported and radiated). Nevertheless, it can be concluded that such relatively small amount of radiation does not have any noticeable deteriorating effect on the cells.

4.4 Lifetime modelling

The degradation rates identified throughout sections 4.1 and 4.2 can be then used in a combination of the additive lifetime model, presented in Eq. (5) and (6), to predict the battery degradation. The verification shall be done on a measurement, that was not used for its parametrization, in order to obtain not biased results. Thus, the degradation rates identified in 4.2.1 – cycling temperature dependence are omitted, and the test at 25°C is actually used as the verification scenario.

The predicted and measured values are shown in Fig. 10. The resulting root-mean-square-error is 0.69% and 0.81% for the capacity and the resistance, respectively. Thus, the considered lifetime model can be considered valid and accurate for the enveloped conditions.

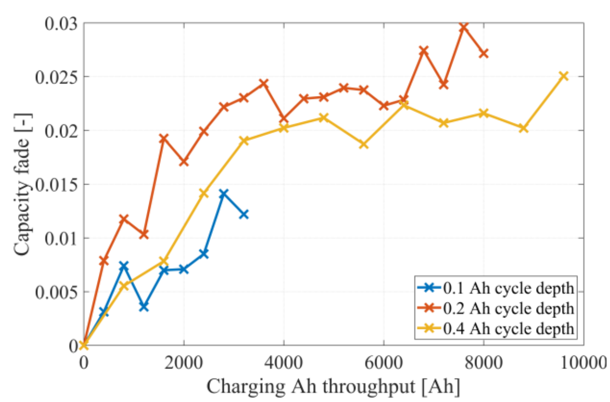

Fig. 7. Degradation results of capacity fade for the cycling aging dependent on cycle depth. The cells were cycled by the 3 A constant current at room temperature.

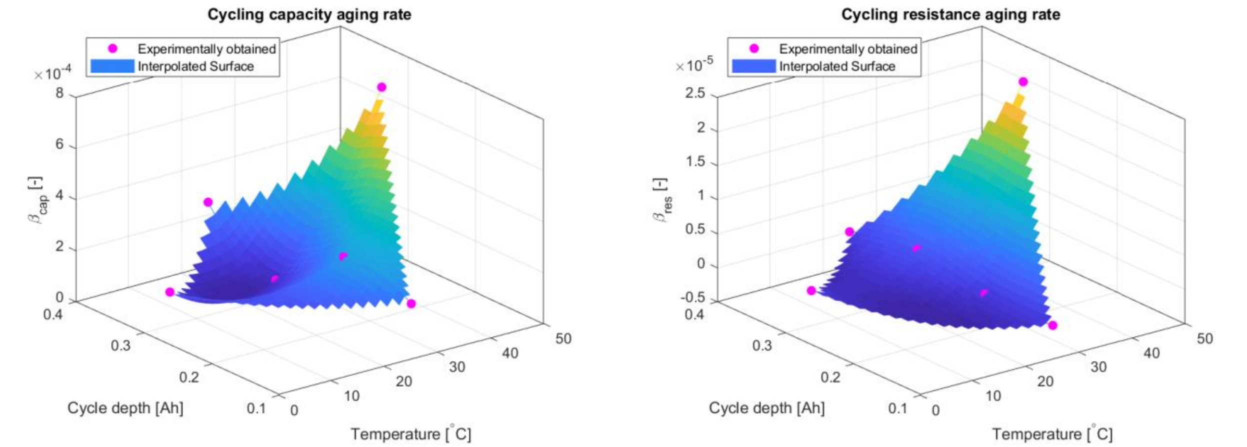

(a) (b)

Fig. 8. Degradation (a) capacity and (b) resistance rate for cycling aging in relation to cycle depth and temperature.

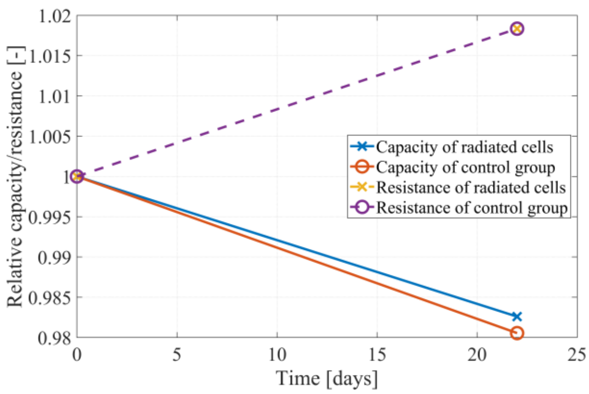

Fig. 9. Capacity and resistance evolution of radiated and not radiated cells.

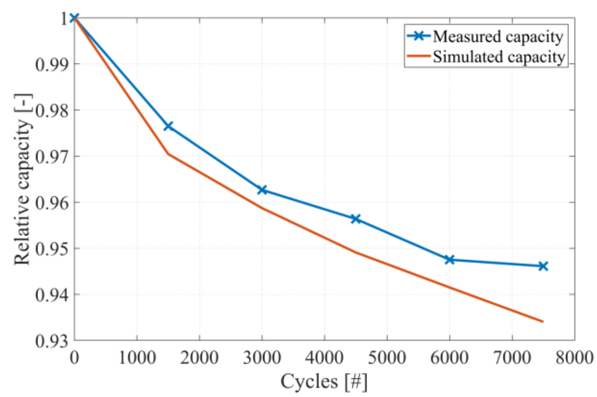

(a)

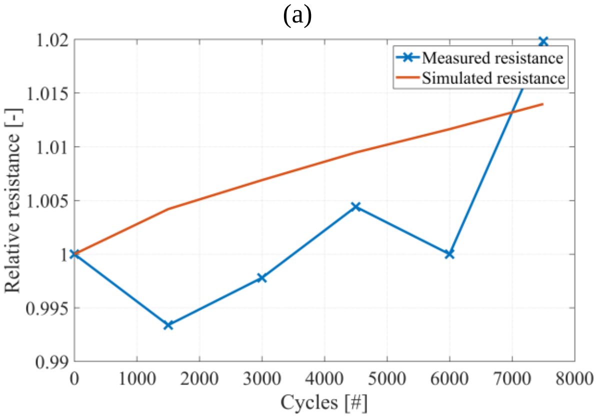

(b)

Fig. 10. Predicted and measured (a) capacity and (b) resistance for the SMP cycling at 25°C.

4. Conclusions

A methodology for testing and lifetime modelling of Li-ion battery cells used in nano-satellite/CubeSat was presented in this paper. The lifetime testing conditions were designed in order to be close to the application use and to cover the relevant range. From the study, it is clear that the major influencing degradation factor is the temperature, both for cycling and calendar aging. Generally, the cells were less sensitive to SOC and cycle depth in the selected range. However, calendar aging at various SOC revealed that the capacity and resistance change throughout degradation are independent. Thus, to consider only the resistance is not suitable as a direct indicator for the cell's capacity during its lifetime. Based on the identified degradation rates, a lifetime model was formed, and it was verified against experiment results, with a root-mean-square-error of 0.69% and 0.81% for the capacity and the resistance, respectively. A potential influence of average cycle SOC and current rate was also observed. Thus, their inclusion into the testing and modelling can lead to improved accuracy of interpretations and the lifetime model.

Acknowledgements

This work was supported by Innovation Fund Denmark (Grant No: 8054-00027B).

References

[1] V. Knap, L. K. Vestergaard, and D.-I. Stroe, “A Review of Battery Technology in CubeSats and Small Satellite Solutions,” *Energies*, vol. 13, no. 16, p. 4097, Aug. 2020.

[2] N. Omar *et al.*, “Lithium iron phosphate based battery – Assessment of the aging parameters and development of cycle life model,” *Appl. Energy*, vol. 113, pp. 1575–1585, Jan. 2014.

[3] K. Takeno, M. Ichimura, K. Takano, and J. Yamaki, “Influence of cycle capacity deterioration and storage capacity deterioration on Li-ion batteries used in mobile phones,” *J. Power Sources*, vol. 142, no. 1, pp. 298–305, 2005.

[4] D.-I. Stroe, M. Swierczynski, S. K. Kaer, E. M. Laserna, and E. S. Zabala, “Accelerated aging of Lithium-ion batteries based on electric vehicle mission profile,” in *2017 IEEE Energy Conversion Congress and Exposition (ECCE)*, 2017, vol. 2017-Janua, pp. 5631–5637.

[5] D.-I. Stroe, M. Swierczynski, A.-I. Stan, R. Teodorescu, and S. J. Andreasen, “Accelerated Lifetime Testing Methodology for Lifetime Estimation of Lithium-Ion Batteries Used in Augmented Wind Power Plants,” *IEEE Trans. Ind. Appl.*, vol. 50, no. 6, pp. 4006–4017, Nov. 2014.

[6] Y. Borthomieu, “Satellite Lithium-Ion Batteries,” in *Lithium-Ion Batteries*, Elsevier, 2014, pp. 311–344.

[7] ESA-ESTEC, “Space engineering Li-ion battery testing handbook (ECSS-E-HB-20-02A),” no. October. ESA Reuqirements and Standards Division, pp. 1–31, 2015.

[8] D. Prevot, Y. Borthomieu, E. Ligneel, R. Hague, J.-P. Peres, and C. Cenac-Morthe, “Performances of Saft Lithium-Ion Cells in LEO Cycling,” *E3S Web Conf.*, vol. 16, no. 1, May 2017.

[9] C. Jacky, R. Stephane, and B. Yannick, “VES16 battery range: Every space application has a VES16 solution,” in *2019 European Space Power Conference (ESPC)*, 2019.

[10] R. Buckle and S. Roberts, “Review of Commercial Cells For Space Applications,” *E3S Web Conf.*, vol. 16, no. 1, p. 17006, May 2017.

[11] A. Clarke and R. Buckle, “Identification of COTS Cells to Meet Space Market Segment Requirements,” in *2019 European Space Power Conference (ESPC)*, 2019, pp. 1–4.

[12] R. Buckle, “Life Testing of COTS Cells for Optimum Battery Sizing,” in *2019 European Space Power Conference (ESPC)*, 2019, pp. 1–7.

[13] V. Knap, L. K. Vestergaard, and D. Stroe, “Towards Validation of Battery Mission Lifetime for Nano-satellites: Fast, Cheap and Accurate Through a Representative Mission Profile,” in *2019 European Space Power Conference (ESPC)*, 2019, pp. 1–5.

[14] J. Schmalstieg, S. Käbitz, M. Ecker, and D. U. Sauer, “A holistic aging model for Li(NiMnCo)O2 based 18650 lithium-ion batteries,” *J. Power Sources*, vol. 257, pp. 325–334, Jul. 2014.

[15] J. Schmitt, A. Maheshwari, M. Heck, S. Lux, and M. Vetter, “Impedance change and capacity fade of lithium nickel manganese cobalt oxide-based batteries during calendar aging,” *J. Power Sources*, vol. 353, pp. 183–194, 2017.

[16] H. Aung, J. J. Soon, S. T. Goh, J. M. Lew, and K.-S. Low, “Battery Management System With State-of-Charge and Opportunistic State-of-Health for a Miniaturized Satellite,” *IEEE Trans. Aerosp. Electron. Syst.*, vol. 56, no. 4, pp. 2978–2989, Aug. 2020.